Spatiotemporal dynamics of optically generated electron-hole excitations in single-walled carbon nanotubes

Grönqvist, Johanna; Hirtschulz, M.; Knorr, A.; Lindberg, Markus

Published in:
Physical Review B - Condensed Matter and Materials Physics

Published: 01/01/2010

Document Version
Final published version

Spatiotemporal dynamics of optically generated electron-hole excitations in single-walled carbon nanotubes

J. H. Grönqvist,[1] M. Hirtschulz,[2] A. Knorr,[2] and M. Lindberg[1]
[1]*Institutionen för fysik, Åbo Akademi, Porthansgatan 3, 20500 Åbo, Finland*
[2]*Institut für Theoretische Physik, Technische Universität Berlin, 10623 Berlin, Germany*
(Received 1 June 2009; revised manuscript received 7 December 2009; published 15 January 2010)

A method for studying spatially and temporally resolved many-body dynamics of charge carriers in carbon nanotubes is presented. We derive coherent, spatially inhomogeneous Bloch equations for charge-carrier dynamics in an optically excited carbon nanotube. By solving the equations of motion numerically under spatially inhomogeneous excitation conditions, we also demonstrate a striking difference in carrier drift velocity for excitation at the exciton resonance and above the band edge.

DOI: 10.1103/PhysRevB.81.035414 PACS number(s): 78.66.−w, 42.50.Wk

I. INTRODUCTION

Since their discovery, the extraordinary mechanical, electronic, and optical properties of carbon nanotubes (CNTs) have attracted a lot of scientific interest. The importance of excitonic and correlation effects on the optical properties of these nanoscale systems has been supported by several theoretical and experimental investigations.[1–9] Nonetheless, only a few measurements with spatial resolution have been performed.[10,11] Through recent progress in near-field spectroscopy, local optical properties of CNTs have become experimentally accessible. These measurements are important to understand the origins of photoluminescence and carrier mobility in these quasi-one-dimensional systems.[12] Recently, spatiotemporal dynamics have been studied also in metal-semiconductor nanostructures.[13] In this work, we present a theoretical study of spatially inhomogeneous optical excitation and subsequent spatiotemporal dynamics of excited charge carriers in CNTs, similar to Ref. 14 for multiple quantum-well structures. We focus on the coherent motion of charge carriers in a carbon nanotube, with the carriers generated in a standing-wave light field.

The paper is organized as follows: in Sec. II we introduce the model many-body Hamiltonian and present the dynamical equations of motion derived in the Hartree-Fock approximation. The solutions of the equations of motion are presented in Sec. III, where we separately discuss the results for excitonic and continuum excitations. Finally, in Sec. IV, we give a brief summary of the results and comment on their validity and consequences.

II. MODEL

A. Hamiltonian

A single-layer carbon nanotube constitutes a regular graphene layer rolled into a tube. The investigated configuration is schematically illustrated in Fig. 1. The light field applied to the nanotube forms a standing wave in a resonator, thus providing spatially inhomogeneous excitation conditions. The system is described by the Hamiltonian $\hat{H}=\hat{H}_0+\hat{H}_{\text{el-el}}+\hat{H}_{\text{el-light}}$, where $\hat{H}_0$ describes the free motion of the electrons in the carbon atom lattice, $\hat{H}_{\text{el-el}}$ the interaction between the electrons, and $\hat{H}_{\text{el-light}}$ the dipole interaction between the light field and the electron system. For the many-body description of the electron system of the carbon nanotube we use the second-quantized formalism. The single-particle states used are classified according to band index and lattice vector. By assuming an infinitely long, finite radius nanotube, the lattice vector $\boldsymbol{k}$ decomposes into a continuous component k parallel to the tube axis, and a discrete component m/R perpendicular to the tube axis, $\boldsymbol{k}=k\hat{\boldsymbol{e}}_{\parallel}+\frac{m}{R}\hat{\boldsymbol{e}}_{\perp}$, where m is an integer and R is the tube radius. The discrete nature of the perpendicular component corresponds to a subband formation in the single-particle energy spectrum.[1] The subbands are indexed by the integer m. The fermion creation and annihilation operators are indexed as $\hat{a}_k^{bm}$, where b is the band index. The separate contributions of the many-body Hamiltonian take the form

$$\hat{H}_0=\sum_{bkm}E_b(\boldsymbol{k})\hat{a}_k^{\dagger bm}\hat{a}_k^{bm}, \tag{1}$$

$$\hat{H}_{\text{el-el}}=\frac{1}{2}\sum_{mm'bb'kp,q\neq 0}V(k,p,q)_{mm'}\hat{a}_{k+q}^{\dagger bm}\hat{a}_p^{\dagger b'm'}\hat{a}_{p+q}^{b'm'}\hat{a}_k^{bm}, \tag{2}$$

$$\hat{H}_{\text{el-light}}=-\mathcal{E}(t)\sum_k[d(k)\hat{a}_k^{\dagger \text{v}\mu}\hat{a}_{k-Q}^{\text{c}\mu+1}+d(k)^*\hat{a}_k^{\dagger \text{v}\mu+1}\hat{a}_{k-Q}^{\text{c}\mu}+d(k)\hat{a}_k^{\dagger \text{v}\mu}\hat{a}_{k+Q}^{\text{c}\mu+1}+d(k)^*\hat{a}_k^{\dagger \text{v}\mu+1}\hat{a}_{k+Q}^{\text{c}\mu}]+\text{H.c.} \tag{3}$$

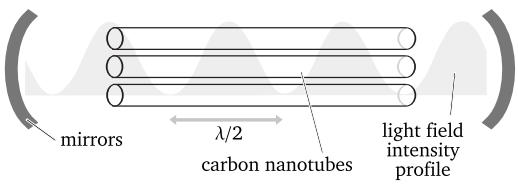

FIG. 1. Schematic representation of the experimental setup, showing the orientation the standing-wave-field modulation in relation to the carbon nanotube axis. The light polarization is perpendicular to the nanotube axis.

In the electron-light interaction, the spatial dependence of the field $E(x,t)=2\mathcal{E}(t)\cos(Qx)$ is included via the nonzero photon momentum Q. The inhomogeneous description of the field envelope allows us to investigate spatial motion explicitly. The field and the electron distributions are assumed homogeneous in the circumferential direction.

We use the tight-binding approximation to determine the $\boldsymbol{k}$ dependence of the single-particle energies, dipole matrix elements, and Coulomb matrix elements. For more details on the tight-binding approximation in carbon nanotubes, see Refs. 1 and 15. The k dependence of the optical dipole matrix elements is given by

$$d(k) \propto e(k,\mu)^* b(k,\mu+1) + e(k,\mu+1) b(k,\mu)^*, \tag{4}$$

where $e(k,m)=\exp\{i \arg[\Sigma_n e^{i(k\hat{\boldsymbol{e}}_\parallel + m/R\hat{\boldsymbol{e}}_\perp)\cdot \boldsymbol{b}_n}]\}$ and $b(k,m)=\Sigma_n \boldsymbol{b}_{n\parallel} e^{i(k\hat{\boldsymbol{e}}_\parallel + m/R\hat{\boldsymbol{e}}_\perp)\cdot \boldsymbol{b}_n}$. The Coulomb matrix elements are given by

$$V(k,p,q)_{m,m'} = V_q^{\mathrm{R}} |G(q)|^2 \frac{1+e(k+q,m)^* e(k,m)}{2} \times \frac{1+e(p,m')^* e(p+q,m')}{2} \tag{5}$$

with the weight functions V_q^{R} and $G(q)$ as in Ref. 6. The Coulomb interaction in this form causes transitions between k states in a band. Transitions between bands or subbands are considerably weaker than the transitions we account for.[16]

In the situation depicted in Fig. 1, the polarization of the light is perpendicular to the nanotube axis. We use this geometrical setup to get the light momentum (directed perpendicularly to the modulation axis) to interact with the continuous component of the electron momentum. This limits our options to using the weakly absorbing perpendicular polarization.[17,18] The fenomena we study are, however, not dependent on a high absorption and should be available whenever any exciton peak occurs. Recent studies have indicated the existence of exciton peaks in the cross-polarized setup.[19–23] For this polarization geometry, the lowest allowed optical transitions are the ones between the lowest subband (μ) in the valence (conduction) band and the second lowest ($\mu+1$) in the conduction (valence) band,[24] indicated by arrows in Fig. 2. We account only for these transitions in the Hamiltonian $\hat{H}_{\text{el-light}}$.

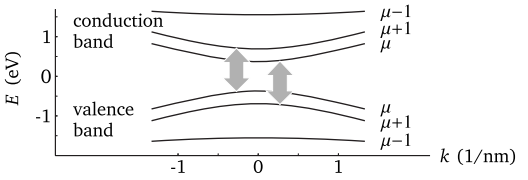

FIG. 2. Tight-binding energy structure of the three lowest subbands in a (14, 0) nanotube. The arrows indicate the lowest allowed optical transitions in the present setup in which the polarization of the light is perpendicular to the nanotube axis.

B. Equations of motion

To investigate the spatially inhomogeneous dynamics of the electron system, we construct equations of motion for the electron degrees of freedom using Heisenberg equations of motion. We use the Hartree-Fock approximation in the Coulomb interaction terms so that the equations of motion for the two-operator expectation values form a closed set of equations.[25] These equations are then further simplified by using the symmetrical subband dispersions and the selection rules of the optical coupling, which lead to two identical and uncoupled transition systems. In this way, we only need equations of motion for the quantities

$$n_{\mathrm{e}}(k,k') \equiv \langle \hat{a}_k^{\dagger \mathrm{c}\mu+1} \hat{a}_{k'}^{\mathrm{c}\mu+1} \rangle,$$

$$n_{\mathrm{h}}(k,k') \equiv \delta_{kk'} - \langle \hat{a}_{-k}^{\dagger \mathrm{v}\mu} \hat{a}_{-k'}^{\mathrm{v}\mu} \rangle,$$

and

$$P(k,k') \equiv \langle \hat{a}_{-k}^{\dagger \mathrm{v}\mu} \hat{a}_{k'}^{\mathrm{c}\mu+1} \rangle \tag{6}$$

for the numerical evaluations. A Fourier transform $n_{\mathrm{e(h)}}(x)=\Sigma_{kk'} e^{i(k-k')x} n_{\mathrm{e(h)}}(k,k')$ gives the electron (hole) distributions in position space. A straightforward derivation leads to the equations of motion

$$\begin{aligned} i\hbar \frac{d}{dt} n_{\mathrm{e}}(k,k') = & -[E_{\mu+1}^{\mathrm{c}}(k) - E_{\mu+1}^{\mathrm{c}}(k')] n_{\mathrm{e}}(k,k') + d(k)\mathcal{E}_0[P(k+Q,k') + P(k-Q,k')] - d(k')^* \mathcal{E}_0[P(k'+Q,k)^* + P(k'-Q,k)^*] \\ & - \sum_p n_{\mathrm{e}}(k,p) \sum_{q\neq 0} V(k',p,q)^*_{\mu+1,\mu+1} n_{\mathrm{e}}(p+q,k'+q) + \sum_p n_{\mathrm{e}}(p,k') \sum_{q\neq 0} V(k,p,q)_{\mu+1,\mu+1} n_{\mathrm{e}}(k+q,p+q) \\ & - \sum_p P(p,k)^* \sum_{q\neq 0} V(k',p,q)^*_{\mu+1,\mu} P(p+q,k'+q) + \sum_p P(p,k') \sum_{q\neq 0} V(k,p,q)_{\mu+1,\mu} P(p+q,k+q)^*, \end{aligned} \tag{7}$$

$$i\hbar\frac{d}{dt}n_{\mathrm{h}}(k,k') = -[E_{\mu}^{\mathrm{v,ren}}(k') - E_{\mu}^{\mathrm{v,ren}}(k)]n_{\mathrm{h}}(k,k') + d(k)\mathcal{E}_0[P(k',k-Q) + P(k',k+Q)] - d(k')^*\mathcal{E}_0[P(k,k'-Q)^* + P(k,k'+Q)^*]$$
$$- \sum_p n_{\mathrm{h}}(k,p)\sum_{q\neq 0} V(k',p,q)_{\mu,\mu}n_{\mathrm{h}}(p+q,k'+q) + \sum_p n_{\mathrm{h}}(p,k')\sum_{q\neq 0} V(k,p,q)^*_{\mu,\mu}n_{\mathrm{h}}(k+q,p+q)$$
$$- \sum_p P(k,p)^*\sum_{q\neq 0} V(k',p,q)_{\mu,\mu+1}P(k'+q,p+q) + \sum_p P(k',p)\sum_{q\neq 0} V(k,p,q)^*_{\mu,\mu+1}P(k+q,p+q)^*, \tag{8}$$

and

$$i\hbar\frac{d}{dt}P(k,k') = -[E_{\mu}^{\mathrm{v,ren}}(k) - E_{\mu+1}^{\mathrm{c}}(k') + \hbar\omega + i\hbar\gamma]P(k,k') - d(k')^*\mathcal{E}_0[\delta_{k,k'+Q} - n_{\mathrm{h}}(k'+Q,k) + \delta_{k,k'-Q} - n_{\mathrm{h}}(k'-Q,k)]$$
$$+ d(k)^*\mathcal{E}_0[n_{\mathrm{e}}(k-Q,k') + n_{\mathrm{e}}(k+Q,k')] - \sum_p P(k,p)\sum_{q\neq 0} V(k',p,q)^*_{\mu+1,\mu+1}n_{\mathrm{e}}(p+q,k'+q)$$
$$- \sum_p P(p,k')\sum_{q\neq 0} V(k,p,q)_{\mu,\mu}n_{\mathrm{h}}(p+q,k+q) - \sum_p [\delta_{k,p} - n_{\mathrm{h}}(p,k)]\sum_{q\neq 0} V(k',p,q)^*_{\mu+1,\mu}P(p+q,k'+q)$$
$$+ \sum_p n_{\mathrm{e}}(p,k')\sum_{q\neq 0} V(k,p,q)_{\mu,\mu+1}P(k+q,p+q). \tag{9}$$

The center frequency of the light pulse is denoted by ω and the Coulomb renormalization of the single-particle energies is given by $E_{\mu}^{\mathrm{v,ren}}(k)=E_{\mu}^{\mathrm{v}}(k)-\Sigma_{q\neq 0}V(k,k,q)_{\mu,\mu}$.

Truncation at the Hartree-Fock level is valid at low carrier densities. In subsequent numerical evaluations, we keep the densities low by exciting the system briefly with a low-intensity electric field. At this level of truncation, no screening or exchange effects are included. Specifically, this also excludes the depolarization effect,[17] which would be relevant for higher carrier densities for our perpendicular polarization setup.

In the equation of motion for the polarization $P(k,k')$, we have added a phenomenological damping term proportional to a decay rate γ. This term is introduced to model damping of the microscopic polarization $P(k,k')$ due to pure dephasing. To simulate dephasing in carbon nanotubes as caused by phonons and exciton-exciton interaction,[26–29] we would need a more thorough description. Here we use the decay rate only to identify the exciton state, as the correlation between the electrons and holes described by P vanishes under influence of the damping.

III. NUMERICAL RESULTS

For the numerical evaluation of Eqs. (7)–(9) we fix the nanotube to be of type (14, 0). The nonchiral (14, 0) tube has bands which are symmetrical with respect to $k=0$ and a tube radius of approximately 5.5×10^{-10} m. Our choice of nanotube type is not expected to affect the results qualitatively.

Linear absorption spectra[6] for the investigated transition are shown in Fig. 3. These spectra are obtained by assuming zero electron and hole populations in Eq. (9), the equation of motion for the polarization. The full spectrum (i.e., Coulomb interaction included) shows a clear excitonic peak (black solid line). Without Coulomb interaction, a band-to-band continuum below the excitonic resonance is observed (gray solid line). The band renormalization shifts this continuum toward higher energies (dashed line) showing the position of the renormalized band. We emphasize that these spectra are calculated in the simplest possible approximation and are shown only to indicate where exciton and continuum states are located in our model system. The absolute positions of the exciton peak and the continuum are of no consequence for the carrier dynamics. For subsequent calculations, the full equations of motion are used.

In the following sections we study the spatiotemporal dynamics of carriers excited by a square light pulse, switched on at $t=0$ and off at $t=20$ fs. As a peak value for the dipole matrix element $d(k=0)\mathcal{E}_0/\hbar$ we use 8.86×10^{-4} ps^{-1}. We solve the equations of motion of Sec. II B numerically, using a Runge-Kutta solver. In analogy with Ref. 30, we would expect excitation in the band to create ballistically moving electrons and holes, whereas electron-hole pairs created in a bound exciton state are expected to move only slowly, due to their hydrogenlike dispersion. Both cases are studied in the following.

A. Exciton dynamics

We choose the center frequency of the light field resonant with the exciton peak in the absorption spectrum. A standing-

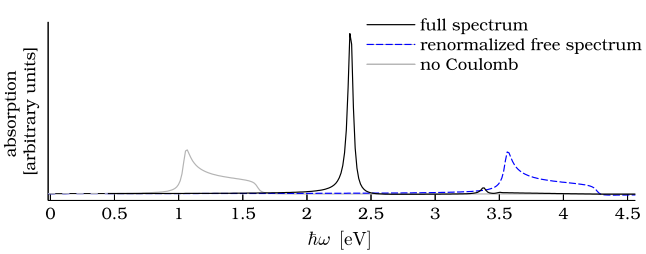

FIG. 3. (Color online) Linear absorption spectra for the transition $(v,\mu)\leftrightarrow(c,\mu+1)$ in a (14, 0) nanotube.

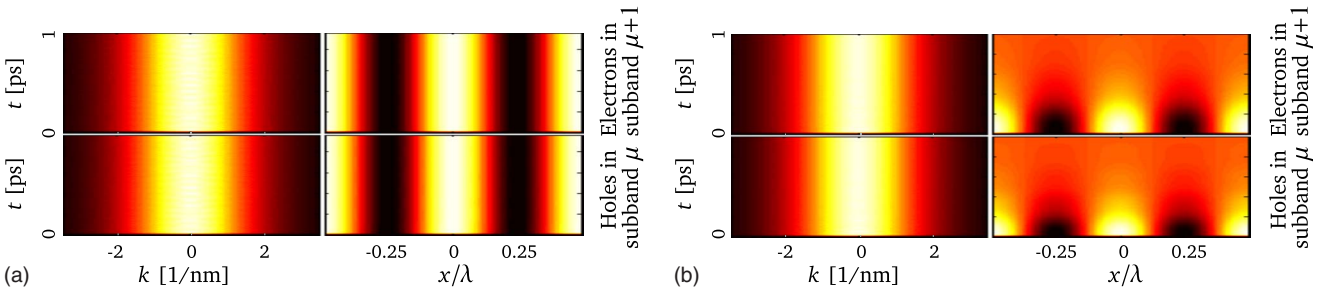

FIG. 4. (Color online) Time dependence of the electron and hole populations in momentum space (k) and position space (x). The center frequency of the exciting pulse is in resonance with the exciton. The pulse is turned off at 20 fs. White indicates the highest density of carriers and black no carriers. (a) shows the results with no dephasing, and (b) the results with a dephasing rate $\gamma=2$ ps^{-1}.

wave pulse is applied in the x direction at $t=0$ and switched off at $t=20$ fs. Figure 4(a) shows the time dependence of the electron and hole populations, Eqs. (7) and (8), up to $t=1$ ps, in both momentum and position representation. The damping constant is here set to zero. Both the momentum distributions and the spatial profiles of the carriers are very stable. The spatial profiles follow the envelope of the standing wave field. Notable is that the excitons do not show observable center-of-mass motion, even if the carrier states contain relatively large momenta.

In Fig. 4(b) we show the corresponding distributions for the same simulation with a damping term present. The value of γ is chosen as 2 ps^{-1} in order to see the effects of the damping on our chosen time scale. We see that the momentum distributions are unaffected by the damping. The spatial profiles, however, are dramatically different. The damping suppresses the Coulomb coupling of electron and hole within the exciton and as a consequence, the spatial profiles spread ballistically. This demonstrates that the immobility in Fig. 4(a) is indeed due to Coulomb coupling.

The slow spreading in Fig. 4(a) is due to both a high exciton mass and low center-of-mass exciton momentum. Also, a contributing but not dominating mechanism is the enhancement of the exciton effective mass as discussed in Ref. 31. To extract further information, one would need to solve the wave function for the 1s exciton and to calculate the corresponding dynamics.

To obtain an estimate for macroscopical quantities such as the diffusion coefficient, a more precise modeling of the scattering processes affecting the exciton is needed. Also, a description of the full exciton dynamics at higher densities requires dynamical inclusion of the next level in the equation of motion truncation hierarchy, i.e., four-operator expectation values,[32] which at present is numerically unfeasible for the inhomogeneous case.

B. Unbound carrier dynamics

To study the dynamics and carrier excitations related to band-to-band transitions in the absorption spectrum, we choose the center frequency about 0.4 eV above the edge of the band gap. All other pulse parameters are the same as for the excitation at the exciton resonance and we neglect the dephasing rate. We solve the same equations as in Sec. III A, i.e., full Coulomb interaction and the corresponding renormalization is included.

The results are shown in Fig. 5 as a function of time. The momentum distribution is doubly peaked since we excite above the band minimum. In position space, we see that the carriers are created at the field maxima, as in the excitonic transition case. Because of the double peak in the momentum distribution, each initial peak in position space will split into two parts, moving ballistically in opposite directions. The chequered pattern shown in the figures is formed when the wave packets from one initial peak meet those originating at other field maxima.

The electrons and the holes move with different speeds since the effective masses in subbands μ and $\mu+1$ are different. This difference in speed indicates that their motion is not strongly correlated. In the considered case, their motion is dominated by free particle properties. Significant here is that the carriers move ballistically even in the absence of damping, in contrast to the results of Fig. 4. The different excitonic and electron/hole motion in CNTs will also be observed in models with a more detailed and realistic Coulomb interaction since our results show such a clear distinction between both cases.

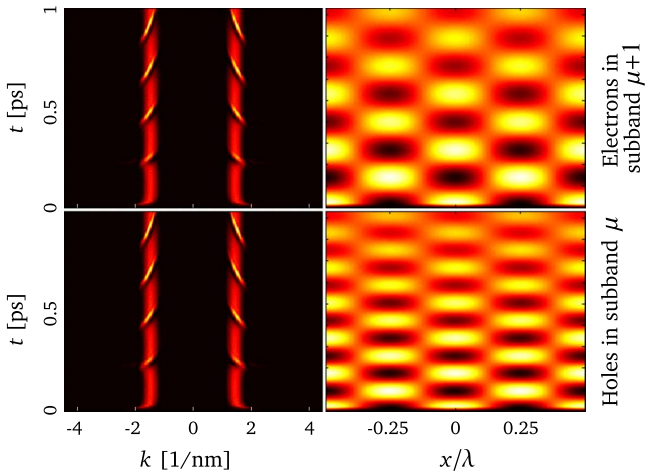

FIG. 5. (Color online) Time dependence of the electron and hole populations in momentum space (left column) and position space (right column). The center frequency of the exciting pulse is tuned to 0.4 eV above the band edge. The pulse is turned off at 20 fs. No dephasing.

IV. SUMMARY AND CONCLUSIONS

We have investigated the coherent dynamics of light generated carriers in a carbon nanotube in the Hartree-Fock approximation. Our results show that carriers created in an excitonic transition do not spontaneously move along the tube on the time scale of a picosecond. The absence of motion is caused by a strong Coulomb correlation between the electrons and holes. Carriers created in a band-to-band transition, on the other hand, move ballistically along the tube. We see that the electrons and holes the band-to-band case move with different speeds, which is consistent with the view that the Coulomb correlations are not as important as in the excitonic transition case. The ballistic motion is expected to slow down if, e.g., scattering by phonons is included.[33] These varying characteristic motions of photogenerated carriers may play an important role in interpreting measurements of electronic conduction in carbon nanotubes.

ACKNOWLEDGMENTS

J.G. acknowledges financial support from the Väisälä Foundation. The Berlin group thanks the Deutsche Forschungsgemeinschaft (Schwerpunktprogramm "Ultrafast Nanooptics") for support.

[1] S. Reich, C. Thomsen, and J. Maultzsch, *Carbon Nanotubes: Basic Concepts and Physical Properties* (Wiley-VCH, Berlin, 2004).
[2] V. Perebeinos, J. Tersoff, and Ph. Avouris, Phys. Rev. Lett. **92**, 257402 (2004).
[3] J. Jiang, R. Saito, G. G. Samsonidze, A. Jorio, S. G. Chou, G. Dresselhaus, and M. S. Dresselhaus, Phys. Rev. B **75**, 035407 (2007).
[4] F. Wang, G. Dukovic, L. E. Brus, and T. F. Heinz, Science **308**, 838 (2005).
[5] T. Ando, J. Phys. Soc. Jpn. **66**, 1066 (1997).
[6] M. Hirtschulz, F. Milde, E. Malić, S. Butscher, C. Thomsen, S. Reich, and A. Knorr, Phys. Rev. B **77**, 035403 (2008).
[7] M. Hirtschulz, F. Milde, E. Malić, C. Thomsen, S. Reich, and A. Knorr, Phys. Status Solidi B **245**, 2164 (2008).
[8] C. D. Spataru, S. Ismail-Beigi, L. X. Benedict, and S. G. Louie, Phys. Rev. Lett. **92**, 077402 (2004).
[9] J. Deslippe, M. Dipoppa, D. Prendergast, M. V. O. Moutinho, R. B. Capaz, and S. G. Louie, Nano Lett. **9**, 1330 (2009).
[10] A. Hartschuh, E. J. Sánchez, X. S. Xie, and L. Novotny, Phys. Rev. Lett. **90**, 095503 (2003).
[11] M. Freitag, J. Tsang, and Ph. Avouris, Phys. Status Solidi B **245**, 2216 (2008).
[12] L. Lüer, S. Hoseinkhani, D. Polli, J. Crochet, T. Hertel, and G. Lanzani, Nat. Phys. **5**, 54 (2009).
[13] M. Reichelt and T. Meier, Opt. Lett. **34**, 2900 (2009).
[14] E. Sherman, R. Abrarov, and J. Sipe, J. Appl. Phys. **104**, 103701 (2008).
[15] R. Saito, G. Dresselhaus, and M. S. Dresselhaus, *Physical Properties of Carbon Nanotubes* (Imperial College, London, 1998).
[16] E. Malić, M. Hirtschulz, F. Milde, M. Richter, J. Maultzsch, S. Reich, and A. Knorr, Phys. Status Solidi B **245**, 2155 (2008).
[17] H. Ajiki and T. Ando, Physica B **201**, 349 (1994).
[18] G. S. Duesberg, I. Loa, M. Burghard, K. Syassen, and S. Roth, Phys. Rev. Lett. **85**, 5436 (2000).
[19] S. Uryu and T. Ando, Phys. Rev. B **74**, 155411 (2006).
[20] H. Zhao and S. Mazumdar, Phys. Rev. Lett. **93**, 157402 (2004).
[21] Y. Miyauchi, M. Oba, and S. Maruyama, Phys. Rev. B **74**, 205440 (2006).
[22] J. Lefebvre and P. Finnie, Phys. Rev. Lett. **98**, 167406 (2007).
[23] K.-C. Chuang, A. Nish, J.-Y. Hwang, G. W. Evans, and R. J. Nicholas, Phys. Rev. B **78**, 085411 (2008).
[24] A. Grüneis, R. Saito, G. G. Samsonidze, T. Kimura, M. A. Pimenta, A. Jorio, A. G. Souza Filho, G. Dresselhaus, and M. S. Dresselhaus, Phys. Rev. B **67**, 165402 (2003).
[25] M. Lindberg and S. W. Koch, Phys. Rev. B **38**, 3342 (1988).
[26] K. Yoshikawa, R. Matsunaga, K. Matsuda, and Y. Kanemitsu, Appl. Phys. Lett. **94**, 093109 (2009).
[27] K. Matsuda, T. Inoue, Y. Murakami, S. Maruyama, and Y. Kanemitsu, Phys. Rev. B **77**, 033406 (2008).
[28] B. F. Habenicht, H. Kamisaka, K. Yamashita, and O. V. Prezhdo, Nano Lett. **7**, 3260 (2007).
[29] D. Abramavicius, Y.-Z. Ma, M. W. Graham, L. Valkunas, and G. R. Fleming, Phys. Rev. B **79**, 195445 (2009).
[30] F. Steininger, A. Knorr, T. Stroucken, P. Thomas, and S. W. Koch, Phys. Rev. Lett. **77**, 550 (1996).
[31] V. Perebeinos, J. Tersoff, and Ph. Avouris, Nano Lett. **5**, 2495 (2005).
[32] M. Kira and S. W. Koch, Prog. Quantum Electron. **30**, 155 (2006).
[33] F. Steininger, A. Knorr, P. Thomas, and S. W. Koch, Z. Phys. B: Condens. Matter **103**, 45 (1997).